Structure and ferroelectric phase transition of vinylidene fluoride–trifluoroethylene copolymers: 2. VDF 55% copolymer

Kohji Tashiro, Kohji Takano, Masamichi Kobayashi, Yozo Chatani and Hiroyuki Tadokoro

Department of Macromolecular Science, Faculty of Science, Osaka University, Toyonaka, Osaka 560, Japan

(Received 31 January 1983; revised 8 March 1983)

Molecular and crystal structure changes in ferroelectric phase transition of vinylidene fluoride–trifluoroethylene (VDF–TrFE) copolymer with a VDF content of 55 mol% have been investigated by X-ray diffraction and infra-red and Raman spectroscopy. As the temperature rises from room temperature to the Curie point of ~60°C, the polar low-temperature phase consisting of all-*trans* chains experiences a first-order transition to the phase of tilted long *trans* segments connected by some skew bonds. At higher temperature this new phase transforms continuously and steeply to the non-polar high-temperature phase, where the molecular structure consists of a random combination of TG, $T\bar{G}$, T_3G and $T_3\bar{G}$ rotational sequences. In the cooling process the high-temperature phase transforms to the cooled phase, which is essentially equivalent to the phase appearing intermediately in the heating process from the low-temperature to the high-temperature phase. The cooled phase gives a tilting X-ray fibre diagram and is found by X-ray analysis to contain an appreciable amount of so-called 60° domain structure. These are well interpreted by a conformational model of tilting *trans* structure containing skew linkages. The tensile stress along the fibre axis causes the transformation from the cooled phase to the low-temperature phase, where the probability of 60° domain structure and the degree of chain tilting are remarkably reduced.

Keywords Vinylidene fluoride–trifluoroethylene copolymers; ferroelectric phase transition; crystal structures; X-ray analyses; infra-red and Raman spectra

INTRODUCTION

Ferroelectric properties of poly(vinylidene fluoride) (PVDF) form I have been widely investigated by such analytical methods as X-ray diffraction[1–3], infra-red[4,5] and Raman[6] spectroscopy, etc., and also by the measurements of electrical properties such as D–E hysteresis loop[7] and polarization switching currents[8–11]. The Curie temperature of the crystal phase transition, characteristic of ferroelectric substances, has also been sought[12–15]. In 1980, it was found by Yagi *et al.*[16–18] that the copolymers of vinylidene fluoride (VDF) and trifluoroethylene (TrFE) monomers exhibit an anomaly in temperature dependence of dielectric, piezoelectric and elastic constants at certain temperatures. For example, in the copolymer sample with VDF molar content 55% (abbreviated as VDF 55% copolymer) the macroscopic dielectric constant ε_3^M exhibits a maximal peak in the vicinity of 60°–65°C, where the macroscopic piezoelectric constant d_{31}^M decreases drastically down to zero. Fukada *et al.*[19–21] interpreted the phenomena thus observed in terms of ferroelectric phase transition between ferroelectric and paraelectric crystal phases. Their experimental results are summarized as follows. (i) The relationship between the electric susceptibility ε_3^M and temperature fits well the so-called Curie–Weiss equation. (ii) Remnant polarization of the poled sample reduces to zero in the vicinity of the transition temperature. (iii) The lattice spacings measured by X-ray diffraction method change steeply near the transition point and the amount of change in spacing Δd is linearly proportional to the square of remnant polarization, indicating the existence of spontaneous deformation induced by the parallel dipole arrays in ferroelectric crystal phase. (iv) Observation of critical slowing down phenomenon for dielectric relaxation time has been made. (v) Anomalous specific heat has been measured. The discovery of ferroelectric phase transition of VDF 55% copolymer may be the first case for organic synthetic polymers.

In order to clarify the transition mechanism in this ferroelectric polymer material, we have investigated the crystal structural changes occurring in the phase transition for the series of VDF–TrFE copolymers by X-ray diffraction and infra-red and Raman spectra. In the previous communication[22] we reported that the transition involves a conformational change between the extended *trans* zigzag form (ferroelectric phase) and the contracted *gauche* form constructed by combination of TG, $T\bar{G}$, T_3G and $T_3\bar{G}$ rotational isomers (paraelectric phase). Such a large conformational change is unique for polymer materials with dipoles connected to each other by strong covalent bonding along the chain axis. It is quite

0032-3861/84/020195-14$03.00

different from the general case of ferroelectric phase transition of ionic low-molecular-weight crystals where only the small atomic displacements or rotations of ionic groups are observed[23]. The detailed structural study on phase transitional behaviours of VDF–TrFE copolymers will and did actually help us to find out the transitional temperature for ferroelectric PVDF form I crystal, as already reported[15]. The transition temperature observed for the VDF–TrFE copolymers approaches the melting point as the VDF content increases to 100%. Then PVDF form I crystal was predicted to experience the ferroelectric phase transition at a temperature close to the melting point[13,17,21]. In fact, from the measurements of the temperature dependence of infra-red spectra and d.s.c. thermograms, the phase transition with a conformational change from TT to $T_3GT_3\bar{G}$ was found at about 175°C or immediately below the melting point[15]. X-ray analysis suggested that the crystal transition of PVDF form I occurs between the polar form I and the anti-polar form III[24,25]. The investigation of structural changes in the phase transition of VDF–TrFE copolymers may also be important for understanding the complicated temperature dependences of their electrical and mechanical properties.

In this paper we will report the details of structural change in the ferroelectric phase transition of VDF 55% copolymer by means of X-ray diffraction and infra-red and Raman spectroscopy. Although Lovinger *et al.*[26,27] recently reported the structural change for VDF 52% copolymer independently of us, the detailed structural analyses have not yet been carried out.

EXPERIMENTAL

Samples

VDF 55% copolymer samples were supplied from Daikin Kogyo Co., Ltd. Unoriented samples were prepared by casting from an acetone solution at room temperature or by quenching the melt into dry ice–methanol freezing agent. Uniaxially oriented samples were obtained by elongating the unoriented samples at room temperature (elongation ratio 300–500%). These samples were annealed at 110°–150°C for several hours.

Measurements

X-ray diffraction measurements were carried out by a photographic method using Ni-filtered Cu K_α radiation from a Rigaku Denki Rotaflex RU200. X-ray fiber diagrams at high temperatures were measured by blowing hot air onto the sample or using a high-temperature X-ray cell under the operation of a temperature controller. The accuracy was about ±1°C at 100°C for the blowing method and ±1°C at 170°C for the high-temperature cell. The reflection intensities of the fiber diagrams obtained by the multiple film method were measured by visual comparison with a standard intensity scale and corrected for the Lorentz polarization factor. The temperature dependence of lattice spacings was measured precisely by a PSPC (position-sensitive proportional counter) system with a sample-to-probe distance of 26.0 cm.

Infra-red absorption spectra were measured with a Japan Spectroscopic Co. A-3 type infra-red spectrophotometer (4000–320 cm^{-1}) and a Hitachi FIS-3 far-infra-red spectrophotometer (400–30 cm^{-1}). The temperature dependence of infra-red spectra was measured using a high-temperature optical cell equipped with KBr windows (4000–400 cm^{-1}) or silicon windows (400–30 cm^{-1}) in the temperature range of 20–180°C.

Raman spectra were measured with a Japan Spectroscopic Co. R-500 double monochromator. The 5145 Å line from an argon ion laser was used as an excitation source. Measurements of Raman spectra at high temperatures were carried out by a blowing method.

RESULTS AND DISCUSSION

Outline of structural changes

X-ray diffraction measurements. In *Figure 1* are shown the X-ray fibre diagrams of uniaxially oriented VDF 55% sample taken at the various temperatures. The right-hand side of the diagram is a schematic illustration. The starting material is prepared by an additional drawing of the uniaxially stretched and annealed sample by a few per cent strain at room temperature, the diagram of which is shown in *Figure 1a*. It is essentially the same as the diagram of PVDF form I[28] and the fiber period is estimated to be 2.55 Å, suggesting the molecular structure of all-*trans* zigzag chains. The crystal phase giving this fibre diagram is called hereafter 'low-temperature phase'. As the temperature rises close to the transition point, the reflection intensities of the low-temperature phase become gradually weak and simultaneously a new X-ray fibre pattern begins to appear, where some equatorial reflections are observed to shift up and down from the horizontal line, i.e. the so-called tilting phenomenon is observed (*Figure 1b*)[29]. As the temperature rises furthermore over the transition point, the X-ray diagram continuously transfers to the pattern of paraelectric 'high-temperature phase' (*Figure 1c*). The tilting phenomenon becomes gradually obscure. The equatorial reflections are sharp but the layer lines are very diffuse with the intensity maximum on the meridional line. Furthermore a new layer line is found in the X-ray diagram of the high-temperature phase, though weak and broad, in the middle between the equatorial and the original first layer line. From the interlayer spacings the fibre period of the high-temperature phase is estimated to be 4.60 Å, confirmed from Weissenberg photography for (00*l*) reflections. The newly observed reflections correspond to the (021) reflection of PVDF form II[28] and (102) and (022) reflections of from III[30,31], suggesting that the molecular chain at high temperature takes a conformation similar to those of forms II and III or the glide-type *gauche* conformation. In the cooling process from the high-temperature phase, the equatorial reflections begin to split again up and down from the horizontal line in the vicinity of the transition temperature (*Figure 1d*) and are frozen in at room temperature (*Figure 1e*). The diagram at room temperature has essentially a pattern characteristic of all-*trans* structure. However it does not agree completely with that of the initial low-temperature phase, but corresponds to the diagram that appeared during the heating process from the low-temperature phase to the high-temperature phase. This phase is called 'cooled phase'. When the sample of the cooled phase is heated again, it transfers to the high-temperature phase continuously and steeply in the vicinity of the transition point. The cooled phase transfers to the low-temperature phase by drawing by a few per cent of strain (*Figure 1a*).

In *Figures 2* and *3* are shown the temperature

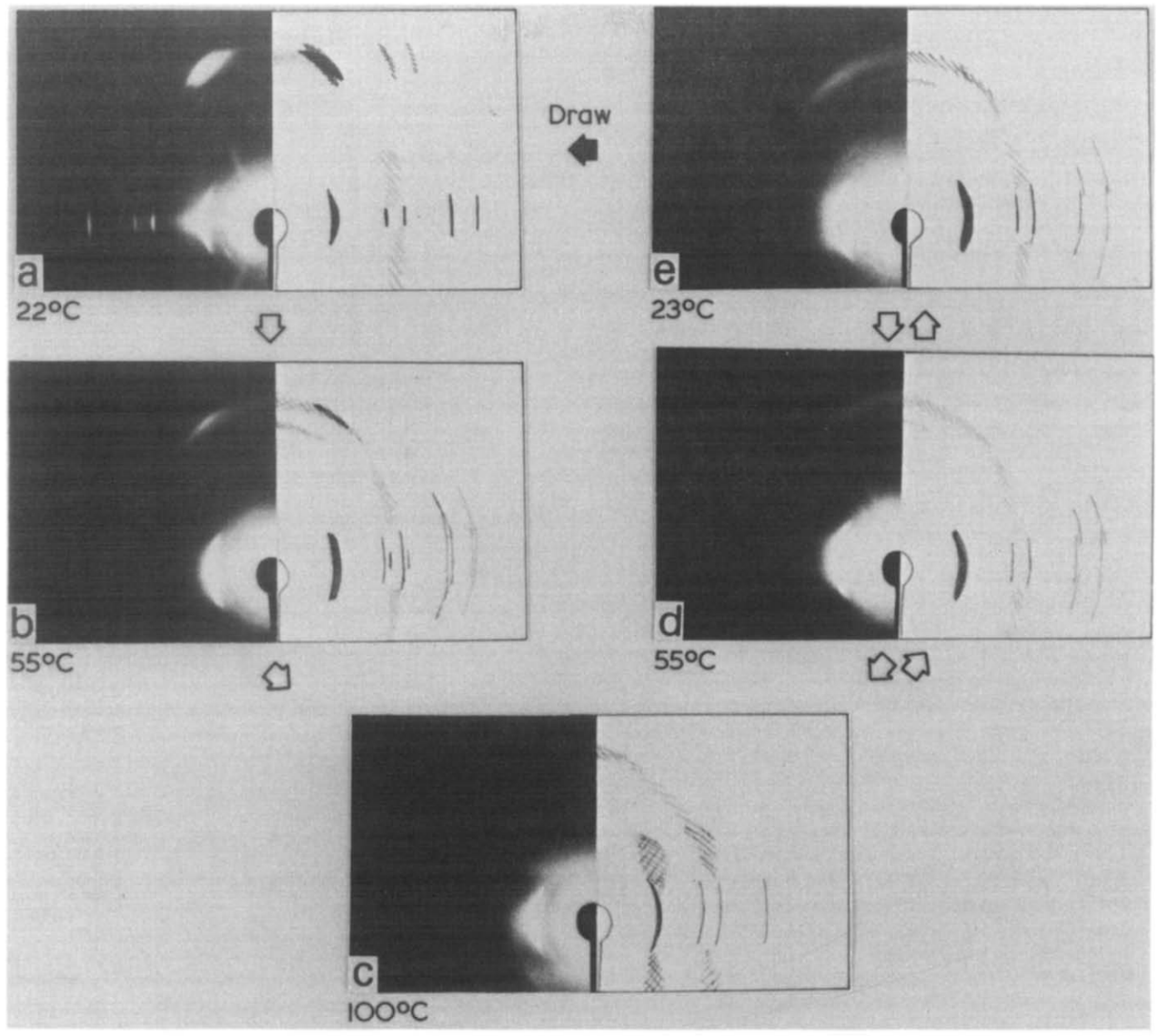

Figure 1 X-ray fibre diagrams of VDF 55% copolymer measured at the various temperatures. Fibre axis is perpendicular to X-ray beam

dependences of lattice spacings for (200) and (110) reflections. These results are essentially the same as those by Lovinger *et al.*[26,27] In the heating process of oriented low-temperature phase, the decrease in reflection intensity and the appearance of new reflections with spacings different from the original ones are observed near the transition point, as already pointed out in *Figure 1*. The new reflections transfer to those of the high-temperature phase continuously but with appreciable shift of position. In the cooling process from the high-temperature phase the spacings steeply approach the values of the cooled phase near the transition temperature. At room temperature the reflection splits into two components with slightly different lattice spacings. They are assigned to (200) and (110) reflections as explained later. The difference in spacing between these two reflections suggests a slight distortion from the hexagonal type lattice. In the case of an unoriented sample (obtained by cooling the melt), the spacings change almost reversibly between the values for the cooled phase and the high-temperature phase. From the results of *Figures 1–3* the phase transitional scheme in VDF 55% copolymer may be described as shown in *Figure 4*.

Infra-red and Raman spectral measurements. In *Figures 5–7* are shown the temperature dependences of polarized infra-red spectra at 1400–30 cm^{-1}. *Figure 8* shows the temperature dependence of relative absorbances for some infra-red bands of unoriented sample. In *Figure 9* are shown the Raman spectra for an unoriented sample measured at room temperature and 81°C. As seen from these figures the bands denoted by arrows exhibit an especially large temperature dependence in the vicinity of the transition point.

In the previous papers[32,33] we carried out the normal coordinates treatments of PVDF forms I, II and III and assigned the infra-red and Raman bands characteristic of long *trans* and *gauche* sequences; for example, 1288 and 350 cm^{-1} for T_m ($m \geqq 4$), 850 cm^{-1} for T_m ($m \geqq 3$), 870 and 614 cm^{-1} for TG, and 811 and 300 cm^{-1} for T_3G. The essential features of spectral patterns of the VDF–TrFE copolymers may be assumed a superimposition of the

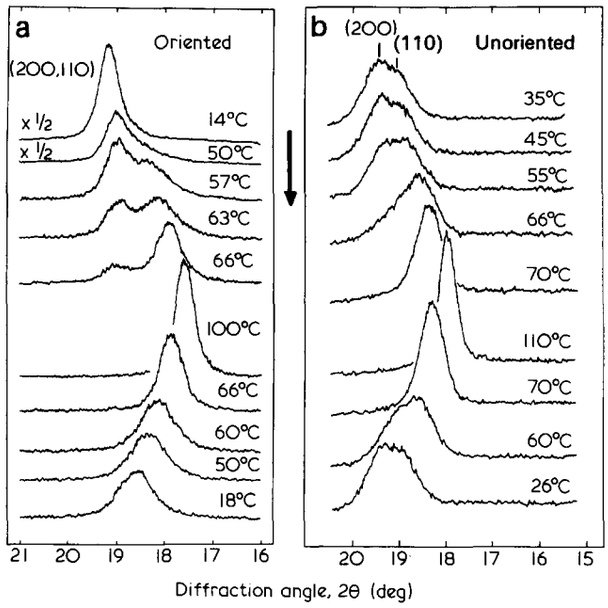

Figure 2 Temperature dependence of X-ray (200) + (110) reflection of (a) uniaxially oriented and (b) unoriented VDF 55% copolymer. The initial sample used in (a) corresponds to the low-temperature phase

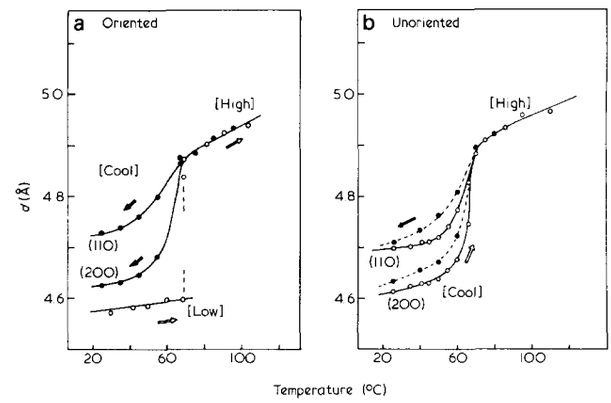

Figure 3 Temperature dependence of lattice spacing $d(200, 110)$ of (a) uniaxially oriented (low-temperature phase) and (b) unoriented VDF 55% copolymer. The reflection positions for the oriented sample were measured from the X-ray photographs taken with a film-to-sample distance of 15 cm because of the difficulty of reading out of the data of *Figure 2a*. The reflection positions for the unoriented sample were measured from *Figure 2b*

spectra of PVDF and poly(trifluoroethylene), though the details are of course different from them. Then, based on the vibrational analyses of PVDF forms I, II and III, we can interpret the temperature dependence of vibrational spectra shown in *Figures 5–9* as follows. As the temperature rises through the transition point, the bands corresponding to the long *trans* sequences (1288 and 850 cm^{-1}) decrease in intensity and those of TG and T_3G sequences (614, 870, 315 cm^{-1}, etc.) increase in turn, indicating the occurrence of a large conformational change from *trans* to *gauche* forms at the transition temperature. Additionally, all through the temperature region below the melting point (~155°C), the infra-red bands show distinct polarization, indicating that the

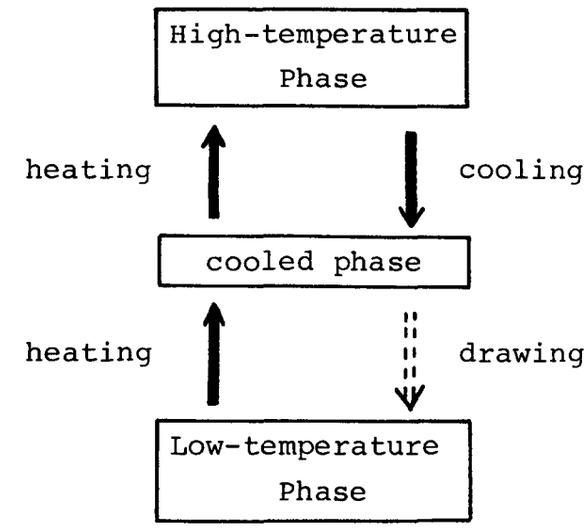

Figure 4 Phase–transitional scheme for VDF 55% copolymer

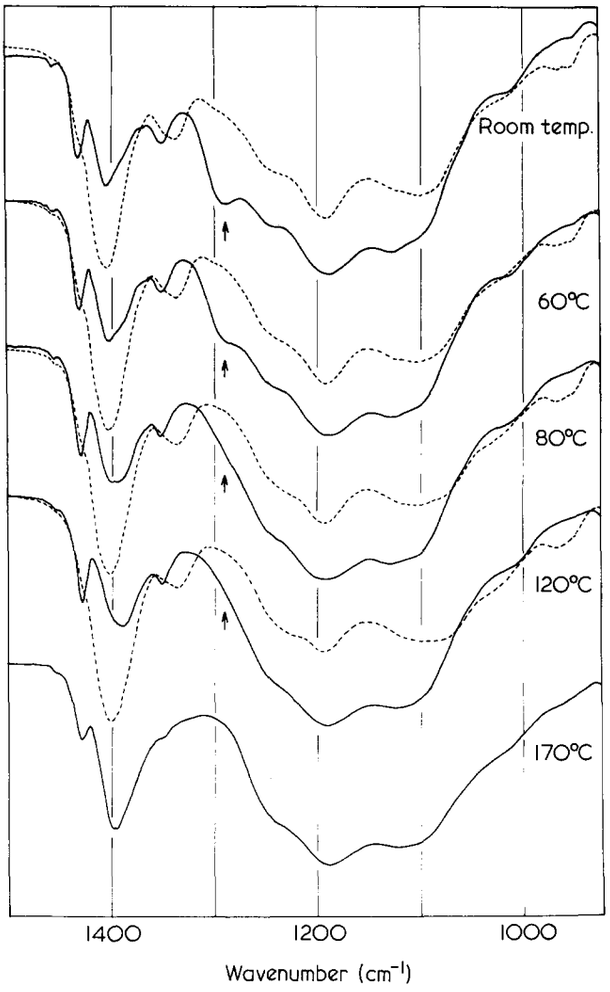

Figure 5 Temperature dependence of polarized infra-red spectra of VDF 55% copolymer in the frequency region 1500–900 cm^{-1}; electric vector of incident infra-red beam ⊥ (——) and // (– – –) to the orientation axis, respectively. The initial sample corresponds to the cooled phase

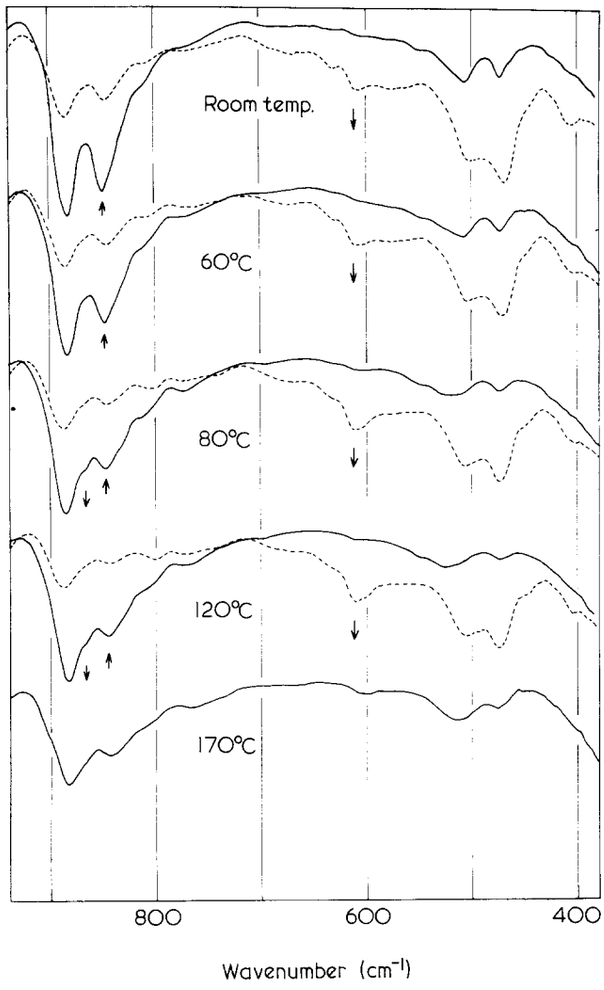

Figure 6 Temperature dependence of polarized infra-red spectra of VDF 55% copolymer in the frequency region 900–400 cm^{-1}. The initial sample corresponds to the cooled phase

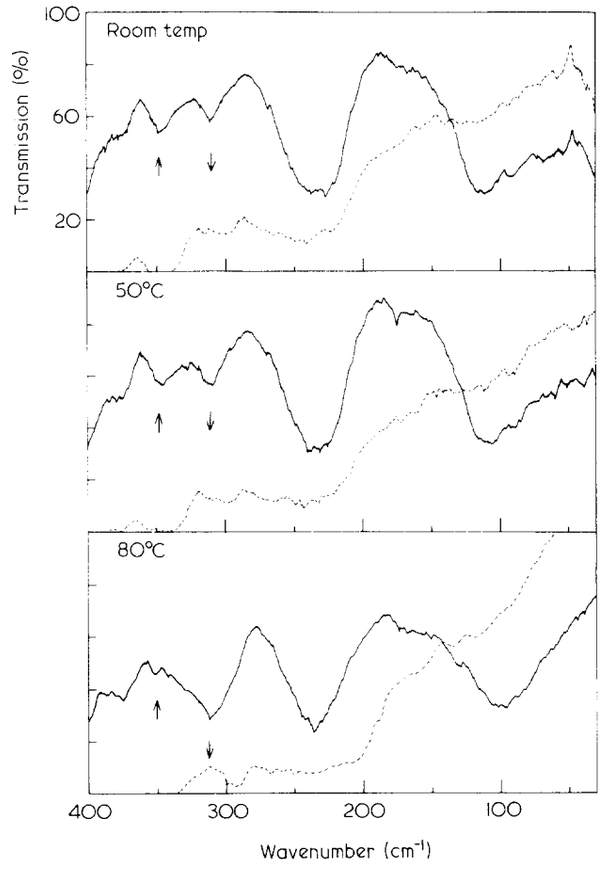

Figure 7 Temperature dependence of polarized infra-red spectra of VDF 55% copolymer in the frequency region 400–30 cm^{-1}. The initial sample corresponds to the cooled phase

conformational change takes place with in the crystalline region. These considerations are consistent with the experimental results of X-ray diffraction measurements as stated above.

From all the experimental results of X-ray diffraction and infra-red and Raman spectroscopy we may say that the ferroelectric phase transition of VDF 55% copolymer is accompanied by a large conformational change between all-*trans* type (fibre period 2.55 Å) and *gauche* type (fibre period 4.60 Å) occurring in the crystalline region.

Structural analyses of three phases of VDF 55% copolymer

Low-temperature phase. The X-ray fibre photograph of the low-temperature phase shown in *Figure 1a* exhibits an essentially similar pattern to that of PVDF form I. In the present case, however, the innermost reflection on the first layer line, (201)+(111), is found to be composed of several reflections having slightly different d spacings to each other. It is not explained simply in terms of an orthorhombic unit cell. In addition these reflections do not lie on a straight layer line but shift up and down from the line, implying a slight degree of tilting phenomenon. As already pointed out, a more notcieable tilting is observed for the cooled phase (*Figure 1e*), which may be comparatively easy to analyse. The low-temperature phase is obtained by stretching the cooled phase by about 5% of strain along the draw direction. Therefore if the tilt line is assumed to be common to these two phases and only a tilt angle is assumed to be different from each other, the analysed results of the tilting phenomenon for the cooled phase will supply useful information for indexing the reflections of the low-temperature phase. The details for the cooled phase will be described later. The following crystallographic parameters for the low-temperature phase could be obtained.:

Monoclinic system

$a=9.12$ Å, $b=5.25$ Å, c (fibre axis) $=2.55$ Å

$\beta=93°$

tilt angle $\phi=3°$ in the tilt plane (130)

The calculated d spacings are compared with the observed values in *Table 1*. The systematic absences of $h+k\neq 2n$ for hkl reflections give a plausible space group of C121 (C_2^3), the ab-plane group of which is common to that of the space group Cm2m (C_{2v}^{14}) of PVDF form I[28].

Because of the essential equivalence of X-ray pattern between PVDF form I and the low-temperature phase of VDF 55% copolymer, we started a calculation of structure factors based on the structural data of PVDF form I crystal[28]: the molecular conformation is essentially of all-*trans* type, but deflected alternately right and left so as to

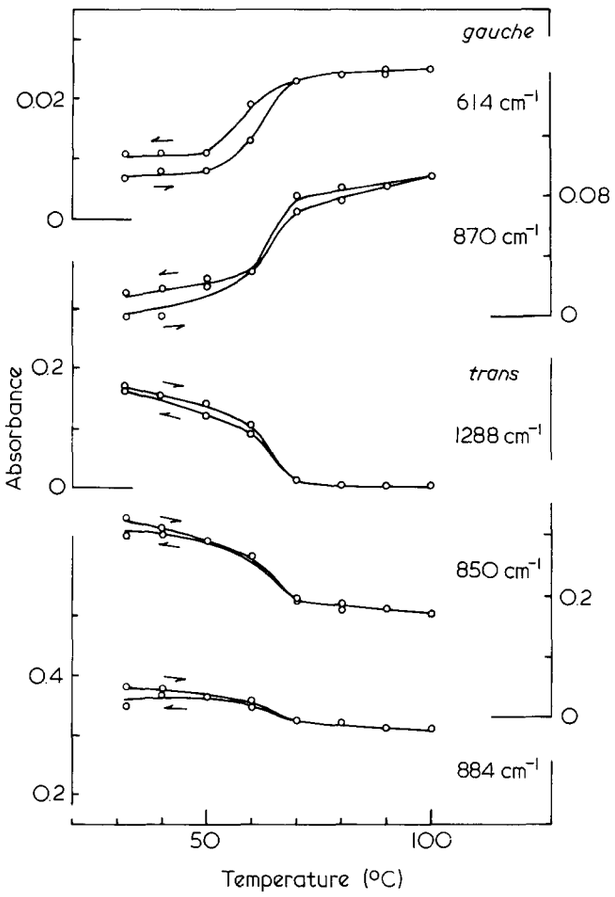

Figure 8 Temperature dependence of infra-red relative absorbances of unoriented VDF 55% copolymer

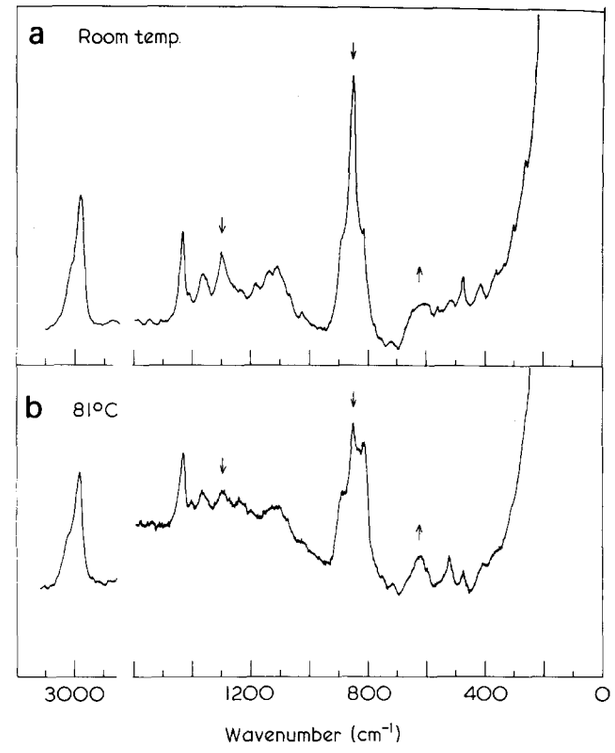

Figure 9 Raman spectra of unoriented VDF 55% copolymer measured at (a) room temperature and (b) 81°C

reduce the steric hindrance between neighbouring non-bonded fluorine atoms. Since the observed fibre period 2.55 Å is half the value for such an alternately deflected zigzag chain model, the mirror imaged molecular chain is also statistically taken into account. The monomer units of VDF and TrFE are considered to be cocrystallizable from the experimental facts that the copolymerization proceeds randomly[34] and that the infra-red bands characteristic of both monomer units increase in intensity after annealing (crystallization-sensitive bands) and show definite polarizations as shown in *Figures 5–7*. Then we took into account the contributions from both monomer units to the X-ray scattering intensity. Practically we estimated the statistical weights of atoms from the various configurations proposed by ^{19}F n.m.r. spectra[34], i.e. the VDF–VDF, VDF–TrFE, TrFE–TrFE monomer sequences and their head-to-tail, head-to-head and tail-to-tail linkages. The result is as follows:

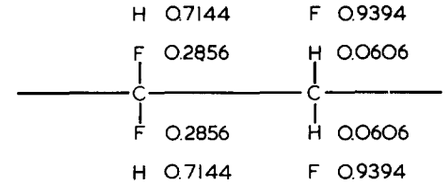

Table 1 Comparison between the calculated and observed *d* spacings and structure factors for the low-temperature phase of VDF 55% copolymer

hkl	d_c (Å)	d_o (Å)	$\sqrt{I_o}^a$	$\sqrt{I_c}$ (1)^b	$\sqrt{I_c}$ (2)^b
200	4.55	4.55	80.9	74.3	82.2
110	4.55				
310	2.63	2.63	15.5	30.1	24.5
020	2.63				
400	2.28	2.28	12.9	14.3	12.3
220	2.28				
510	1.72	1.72	27.4	23.8	22.8
420	1.72				
130	1.72				
600	1.52	1.51	14.9	13.6	14.8
330	1.52				
620	1.31	1.31	6.1	7.1	5.9
040	1.31				
710	1.26	1.27	5.4	7.4	5.4
530	1.26				
240	1.26				
800	1.14	1.14	–	(1.8)	(1.8)
440	1.14				
820	1.04	1.05	–	(3.6)	(3.4)
730	1.04				
150	1.04				
910	0.99	1.00	–	(4.8)	(3.7)
640	0.99				
350	0.99				
201	2.17	2.16	62.5	48.0	49.7
$\bar{2}01$	2.27	2.27			
111	2.19	2.19			
$\bar{1}11$	2.24	2.23			
311	1.79	1.83	16.6	20.7	19.4
$\bar{3}11$	1.87				
021	1.83				
401	1.65	1.70	3.5	6.5	7.6
$\bar{4}01$	1.74				
221	1.67				
$\bar{2}21$	1.72				

Table 1 cont. . . . .

hkl	d_c (Å)	d_o (Å)	$\sqrt{I_o}$[a]	$\sqrt{I_c}$ (1)[b]	$\sqrt{I_c}$ (2)[b]
511	1.39	1.41	–	(3.5)	(2.9)
$\bar{5}11$	1.46				
421	1.40				
$\bar{4}21$	1.45				
131	1.42				
$\bar{1}31$	1.43				
601	1.27	1.30	7.9	6.9	7.2
$\bar{6}01$	1.33				
331	1.29				
$\bar{3}31$	1.32				
621	1.18	1.16	–	(5.7)	(5.8)
$\bar{6}21$	1.19				
041	1.17				
711	1.11	1.13	7.9	7.3	7.6
$\bar{7}11$	1.15				
531	1.11				
$\bar{5}31$	1.15				
241	1.12				
$\bar{2}41$	1.14				
801	1.02	1.04	–	(3.6)	(4.4)
$\bar{8}01$	1.06				
441	1.03				
$\bar{4}41$	1.05				

[a] The observed structure factors $\sqrt{I_o}$ were put on the same scale as the $\sqrt{I_c} = \sqrt{(mF_c^2)}$ by setting $\Sigma k\sqrt{I_o} = \Sigma\sqrt{(mF_c^2)}$, where k is the scale factor and m is the multiplicity. $\sqrt{I_c}$ of the reflections which overlap on X-ray fibre photographs are $\sqrt{(\Sigma mF_c^2)}$. In the calculation of F_c, an isotropic temperature parameter $B = 10$ Å^2 was assumed for all atoms

[b] $\sqrt{I_c}$(1) and $\sqrt{I_c}$(2) are the calculated structure factors for $w = 0\%$ and 14.8%, respectively, where w represents a statistical weight of 60°-rotated zigzag chains in the unit cell of ***Figure 12***

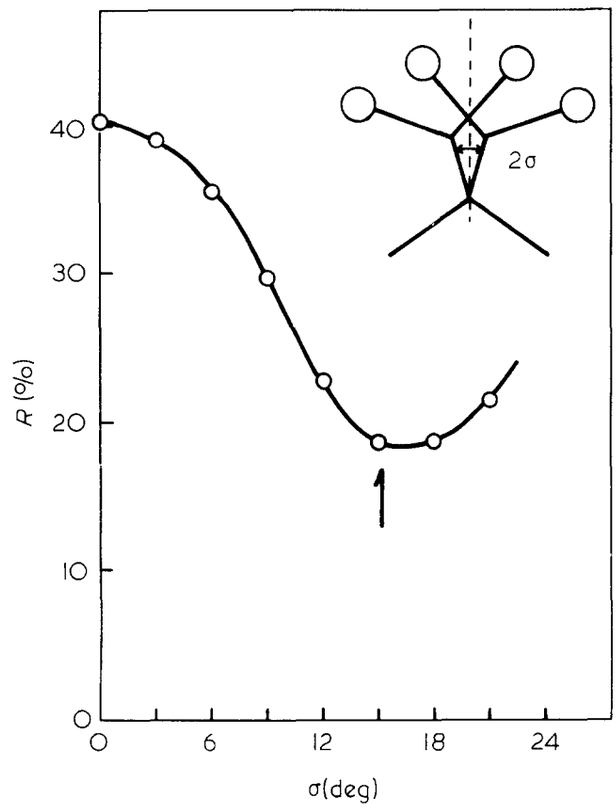

Figure 10 Dependence of R factor on deflection angle σ for the low-temperature phase of VDF 55% copolymer

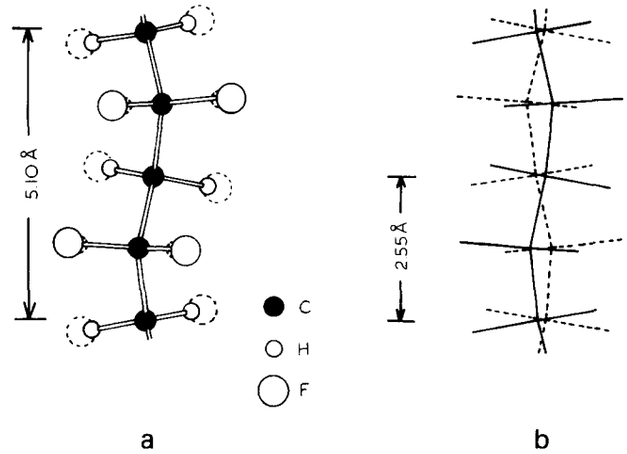

Figure 11 Molecular structure model of the low-temperature phase of VDF 55% copolymer. (a) An alternately deflected zigzag chain and (b) a deflected chain (solid line) and its mirror image (broken line). Fluorine and hydrogen atoms represented by broken lines are also included in some weights

Similarly to the case of PVDF form I, the zigzag chains are packed into the unit cell so that the CF_2 dipoles are parallel along the b-axis. The bond lengths and angles are initially referred to those of PVDF form I[28] and the deflection angle σ of the zigzag chain is used as a variable parameter. In *Figure 10* is plotted the R factor as a function of σ, where

$$R = \sum ||F(\text{obs})| - |F(\text{calc})|| / \sum |F(\text{obs})|$$

and F(obs) and F(calc) are observed and calculated structure factors, respectively. The minimum value of R factor, 20%, is obtained for a deflection angle of about 15°, which is rather large compared with the value 7° of PVDF form I. The reason is now investigated from the viewpoint of the potential energy calculation. In calculation of *Figure 10* the chain deflection is assumed simply to occur so that the CF_2 groups are located on the plane perpendicular to the chain axis, like the case of PVDF form I. Such a way of deflection may not be natural from the structural point of view. The more reasonable way of chain deflection is by internal rotations of skeletal CC linkages. The deflection angle of about 15°, giving a minimal R factor, is made by the following torsional angles:

$$\underset{}{-CH(F)_2-CF(H)_2-CH(F)_2-CF(H)_2-CH(F)_2-}$$
$$\underset{}{-168.7°\quad -155.5°\quad 168.7°\quad 155.5°}$$

In *Figure 11* is shown the molecular model. Such a type of chain deflection displaces the CF_2 and CH_2 groups from the plane perpendicular to the chain axis and generates the distinction between up- and downward chains along the c-axis. Thus, in order to hold the space group symmetry, these chains are statistically placed at one lattice site. The crystal structure model is shown in *Figure 12*, giving an R factor of about 21%. The atomic coordinates are listed in *Table 2*, where the bond lengths are CC = 1.54 Å, CF = 1.34 Å, and CH = 1.09 Å, and the bond angles are FCF = 108.0°, HCH = 112.0°,

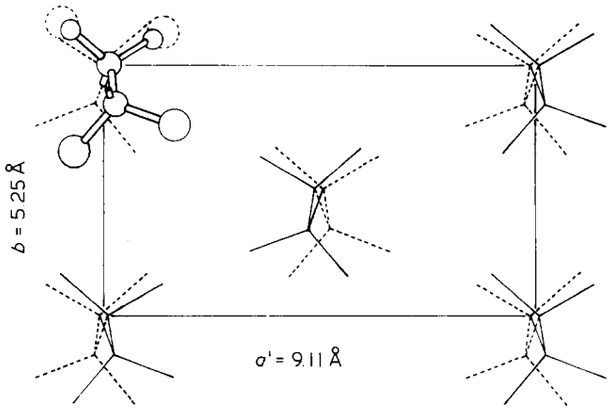

Figure 12 The *c*-axis projection of crystal structural model of the low-temperature phase of VDF 55% copolymer. Fluorine and hydrogen atoms represented by broken lines are also included in some weights

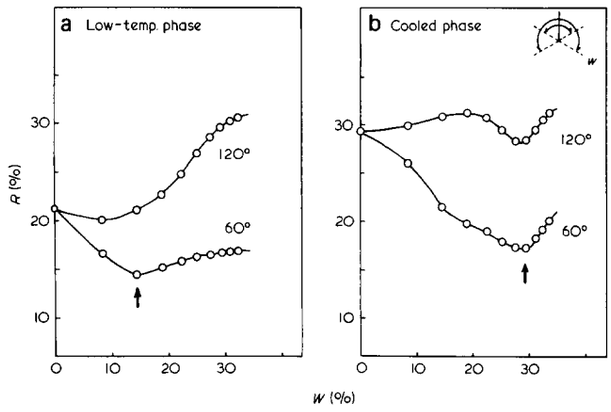

Figure 13 Change of *R* factor with the weight *w* of 60°- and 120°-rotated zigzag chains. (a) The low-temperature phase and (b) the cooled phase

Table 2 Atomic coordinates for the low-temperature phase of VDF 55% copolymer

Atom	*x/a*	*y/b*	*z/c*
C_1	0.009	0.000	0.002
C_2	0.024	0.159	0.509
H_{1a}	0.112	−0.099	−0.045
H_{1b}	−0.081	−0.134	0.039
F_{1a}	0.136	−0.124	−0.048
F_{1b}	−0.101	−0.166	0.056
F_{2a}	0.162	0.248	0.571
F_{2b}	−0.070	0.354	0.476
H_{2a}	0.136	0.230	0.554
H_{2b}	−0.053	0.317	0.476

C(H)C(F)C(H) = 112.0° and C(F)C(H)C(F) = 114.0°[28,30,31].

As shown in *Table 1*, the agreement between the calculated and observed intensities is fairly good. But for the reflection of (020) + (310) the calculated value is only about half the observed one. Such a large difference is also observed in the case of PVDF form I, suggesting that this might be caused from a common origin. In the study of dipole inversion of PVDF form I under high electric field, Kepler and Anderson[1] and Takahashi and Odajima[2] pointed out the possibility of ferroelectric domain structures within the crystallite, where the domains aggregate together with their polar axes making an angle 60° to each other (60° domain structure). Then we calculated the X-ray scattering intensities of the low-temperature phase for the model containing the zigzag chains rotating 60° around the *c*-axis in addition the original zigzag chains in *Figure 12*. In *Figure 13* is shown the *R* factor as a function of statistical weight *w* of 60° or 120° (60° + 60°) rotated chains. The reduction of *R* factor is remarkable for the model including 60°-rotated molecules but not so for the model including 120°-rotated chains. The minimal *R* factor is about 14% for the 60° model with a statistical weight 15%. In *Table 1* are compared the calculated intensities for this model with the observed ones. Although the intensity data of X-ray Bragg reflections may only give the statistically averaged structure of the 0° and ±60° rotated zigzag chains, the coherent rotation of the neighbouring zigzag chains will be more advantageous compared with the case of randomly 0° or ±60° rotated chains from the viewpoint of the packing efficiency into the crystal lattice. That is to say, the present X-ray suggests the possibility of the existence of 60° domain structure within the crystallites of VDF 55% low-temperature phase. The probability of the existence of 60° domain structure is much higher for the cooled phase and will be discussed in relation to the tilting phenomenon and phase transition in a later section.

Summarizing this section, the crystal structure of the low-temperature phase is basically constructed by the parallel arrangements of dipoles of essentially zigzag chains and the possibility of 60° domain structure is considered in a statistical weight of about 15%.

High-temperature phase. Since the number of observed reflections is very small and the layer lines are so broad in the X-ray diagram of the high-temperature phase, it may be difficult at present to analyse the detailed crystal structure. The four equatorial reflections may be indexed by a rectangular unit cell of a hexagonal type:

$$a' = 9.75 \text{ Å}, \quad b' = 5.63 \text{ Å}, \quad a'/b' = \sqrt{3} \quad \text{at } 80°\text{C}$$

The calculated and observed *d* spacings are compared in *Table 3*. As mentioned before, the fibre period of the high-

Table 3 Comparison between the calculated and observed *d* spacings and structure factors for the high-temperature phase of VDF 55% copolymer

hkl	d_c (Å)	d_o (Å)	$\sqrt{I_o}$	$\sqrt{I_c}$ [a]
200	4.87	4.88	38.4	35.4
110	4.87			
310	2.81	2.83	3.2	5.1
020	2.81			
400	2.44	2.44	3.0	3.7
220	2.44			
510	1.84	1.85	1.8	2.2
420	1.84			
130	1.84			
600	1.62	–	–	(2.2)
330	1.62			
620	1.41	–	–	(0.9)
040	1.41			

[a] An isotropic temperature parameter B = 15 Å^2 was assumed for all atoms

temperature phase is estimated to be 4.60 Å. The temperature dependence of infra-red spectra suggests that the molecular chain involves TG and T_3G rotational sequences. The fiber period of PVDF form II ($TG\bar{T}\bar{G}$) is 4.62 Å[28] and that of form III ($T_3GT_3\bar{G}$) is 9.23 Å = 2 × 4.62 Å[30,31]. The statistical average of these two isomeric sequences or random combinations of rotational isomeric sequences of TG, $T\bar{G}$, T_3G and $T_3\bar{G}$ gives a fibre period of 4.62 Å as shown in *Figure 14*, consistent with the X-ray value. It should be noted that our conformational model of random TG and T_3G sequences is essentially based on the glide type because the X-ray fibre pattern becomes more similar to that of PVDF as the VDF monomer content increases to 72–100%[24].

In *Figure 14* is also illustrated the crystal structural model where the molecular chains are packed in a statistically disordered fashion and the net polarization of the crystal vanishes. The packing of the molecules is comparatively good. But, for such a static structural model, the agreement between the observed and calculated X-ray intensities is not so good. As suggested from the dielectric relaxation measurements[21], the thermal rotational motion of chains around the chain axis may be remarkable at high temperature. Time-averaged molecular structure for such a kind of rotator phase may be approximated by the model constructed by a collection of rings, which are the locus generated by rotating all the atoms about the chain axis, as illustrated in *Figure 15*. Such a model of rotator phase may be consistent with the Fourier synthesized electron density map (*Figure 16*) which is calculated from the observed X-ray reflection intensities under an appropriate assumption for the phase angles; an almost isotropic electron density distribution is found in the equatorial plane of the high-temperature phase, different from the case of the polar low-temperature phase. The structure factor $F(R)$ for the model of *Figure 15* is given by:

$$F(R)=\sum_j f_j \exp(2\pi i l z_j/c) J_0(2\pi R r_j)$$

where the f_j and (x_j, y_j, z_j) are the atomic scattering factor and coordinates of the jth atom, respectively, and $r_j=\sqrt{(x_j^2+y_j^2)}$. R is the radius of the cylindrical coordinate in the reciprocal lattice, l is the index for the lth layer reflections, and J_0 is the zeroth-order Bessel function. The molecular parameters utilized in the calculation of structure factors are as follows; bond length CC = 1.54 Å, CF = 1.34 Å, CH = 1.09 Å, bond angles CCC = 114.0°, HCH = 112.0°, FCF = 111.0°, CCH = CCF = 108.0°, and internal rotation angles of skeletal sequences are *trans* = 180.0° and *gauche* = 57.0°. The calculated X-ray intensities for the model are

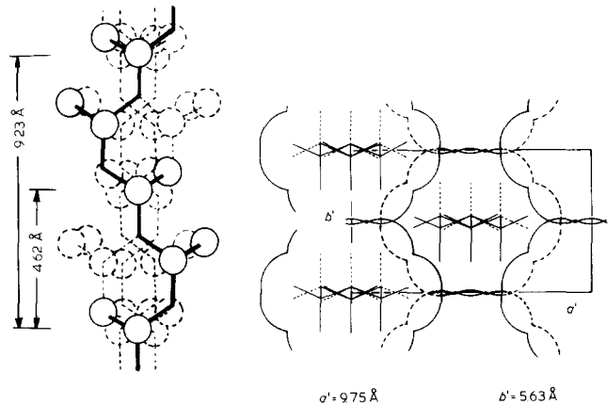

Figure 14 Molecular and crystal structural models for the high-temperature phase of VDF 55% copolymer. For simplicity of illustration the $T_3GT_3\bar{G}$ molecular model is packed in the unit cell

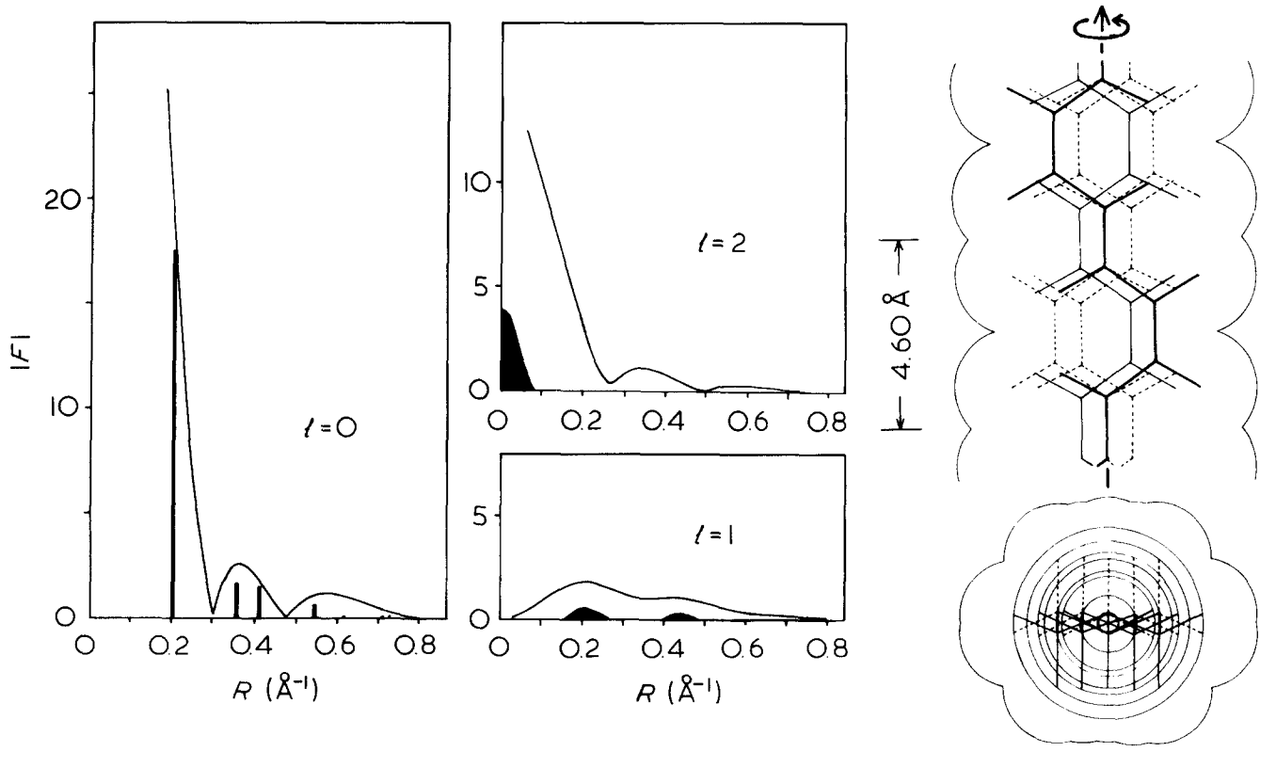

Figure 15 A comparison between observed and calculated X-ray structure factors for a molecular chain constructed by a collection of rings which are generated by rotating a conformational model of *Figure 14*

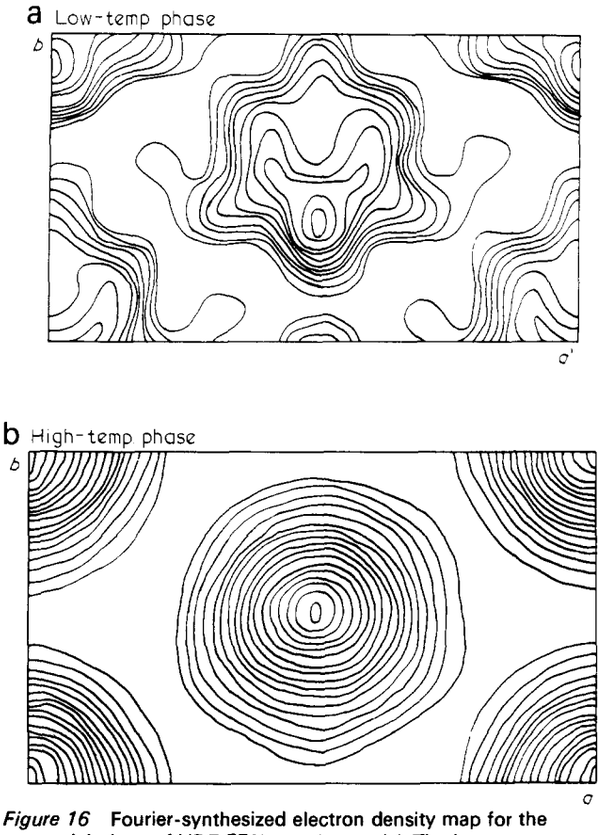

Figure 16 Fourier-synthesized electron density map for the equatorial plane of VDF 55% copolymer. (a) The low-temperature phase and (b) the high-temperature phase

compared with the observed ones in *Figure 15*. The observed intensities for the equatorial reflections indicated by solid bars are in good agreement with the calculated values. In *Table 3* are compared the observed and calculated intensities for equatorial reflections; the R factor is about 13%. For the first and second layers the calculated intensity maxima correspond well to the observed positions, though the quantitative comparison may be difficult because of the broadness of the observed reflections.

From these considerations the most plausible structure model for the high-temperature phase may be described as follows. The chain, constructed by random combination of TG, $T\bar{G}$, T_3G and $T_3\bar{G}$ isomers, experiences an appreciably large thermal motion and then the time-averaged structure becomes equivalent to a kind of rotator phase.

Cooled phase. The cooled phase is obtained by cooling the high-temperature phase down to room temperature. The positional shift of some equatorial reflections from the horizontal line, as shown in *Figure 1e*, can be interpreted uniquely by the tilting phenomenon. Based on the method proposed by Bunn *et al.*[35], we carried out the analysis of tilt diagram and determined the unit cell parameters as follows:

$a=9.16$ Å, $b=5.43$ Å, c (fibre axis) $=2.528$ Å

$\beta=93°$ (assumed)

tilt angle $\phi \simeq 18°$ in the tilt plane (130)

The value of the c-axis is measured by PSPC system with the sample-to-detector distance of 26.0 cm and so it has a high accuracy. In *Figure 17* is shown the comparison of the calculated and observed reflection positions in (a) the fibre diagram and (b) the Weissenberg photograph. The agreement between them is good. The ratio of a to b deviates a little from the value $\sqrt{3}$ of hexagonal unit cell and then the (200) and (110) lattice spacings are slightly different from each other as shown in *Figure 3*. Lovinger *et al.*[26,27] assigned these two reflections to the *trans* and *gauche* crystalline phases; they considered the sample obtained by cooling the high-temperature phase as a mixture of low- and high-temperature phases, but they did so only from the observation of these two reflections. The following experimental facts indicate explicitly that the cooled phase is not a mere mixture of the above-mentioned two phases but principally a unique crystal phase. (i) As shown in *Figure 17*, all the reflections can be indexed by the unit cell parameters described above with tilting phenomenon taken into account. (ii) As shown in *Figure 3*, a large spacing change occurs simultaneously for both the reflections of (200) and (110), suggesting that these changes originate from one overall structural change. (iii) The two reflections under discussion have comparable intensities at room temperature. If these reflections originate from two crystal phases, the relative absorbances of *trans* and *gauche* infra-red bands should also differ appreciably from those of low- and high-temperature phases. But the actual infra-red spectra of the cooled phase are essentially the same as those of low-temperature phase, though slight differences are of course detected as stated later.

The calculation of X-ray scattering intensities was carried out based on the crystal structural model of low-temperature phase (*Figure 12*) because of the similar features in the X-ray diffraction and infra-red spectra. At one lattice site the four kinds of chains are statistically located: the alternately right-to-left and left-to-right deflected chains and their up- and downward setting. At this initial stage the calculated structure factors do not agree so well with the observed ones. The R factor is about 29%. The cooled phase is generated by cooling the isotropic high-temperature phase. When the *trans* dipoles are generated from such isotropic chains, all the dipoles are not necessarily restricted into only one direction; it might be possible that domain structures are generated having their polar axes pointing to other energetically stable 60° directions. Then we calculated the intensities

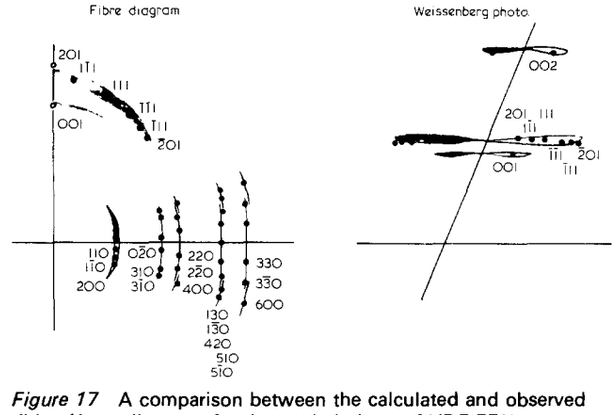

Figure 17 A comparison between the calculated and observed tilting X-ray diagrams for the cooled phase of VDF 55% copolymer

for the model including additional 60°- or 120°-rotated zigzag chains in some statistical weights, as just stated in the case of low-temperature phase. In *Figure 13* is plotted the R factor against the statistical weight of additional chains w; the minimal point of R factor, about 16%, is obtained for $w = 30\%$ of 60°-rotated chains. The existence of 120°-rotated chains is rejected from consideration because of the negative effect on the R factor. The weight $w = 30\%$ is almost twice the value for the low-temperature phase. The ratio of *trans* chains pointing to $-60°$, 0° and $+60°$ directions from the original b-axis is 30 : 40 : 30 which is approximately 1:1:1. In *Table 4* are listed the observed and calculated X-ray intensities for the cooled phase.

In order to proceed further with the analysis we must take into account several characteristic features of the cooled phase. (a) The cooled phase is generated via transformation between *trans* and *gauche* conformations (*Figure 4*). The cooled phase is transferred to the low-temperature phase of all-*trans* chains by drawing about 5% of strain. (b) The fibre period of the cooled phase is almost equal to, but shorter by about 0.5% than, the value for the low-temperature phase. The volume of the unit cell of the cooled phase is about 3% larger than that of the low-temperature phase. (c) The X-ray diffuse scattering is observed, though very weak and broad, in the neighbourhood of the (021) reflection position of the high-temperature phase. (d) The infra-red spectra of the cooled phase is almost the same as those of the low-temperature phase. In *Figure 18* is shown the temperature dependence of relative absorbance of 852 cm^{-1} *trans* band measured for the starting sample of the low-temperature phase. The perpendicular and parallel components of this band for the cooled phase are different in intensity from those of the low-temperature phase, and then the dichroic ratio $D_\parallel/D_\perp$ or the degree of chain orientation along the draw axis is reduced slightly. This result is consistent with the tilting X-ray diagram observed for the cooled phase. But the averaged absorbance of $D_\parallel$ and $D_\perp$ or $(2D_\perp + D_\parallel)/3$, i.e. the

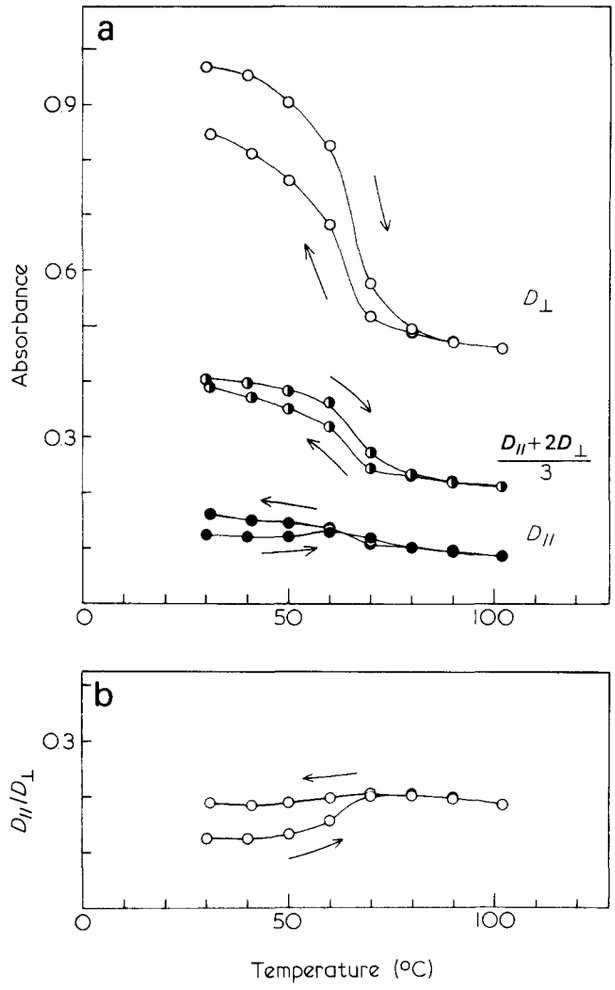

Figure 18 Temperature dependence of infra-red absorbance of 852 cm^{-1} *trans* band of VDF 55% copolymer. (a) The perpendicular ($D_\perp$) and parallel ($D_{//}$) components and their averaged absorbance, $(D_{//}+2D_\perp)/3$, and (b) the dichroic ratio $D_{//}/D_\perp$. The initial sample corresponds to the low-temperature phase

Table 4 Comparison between the calculated and observed structure factors for the cooled phase of VDF 55% copolymer

hkl	$\sqrt{I_o}$ [a]	$\sqrt{I_c}$ [b]
200 / 1$\bar{1}$0	60.1	57.0
110	68.0	63.9
310	7.0	8.5
020	14.8	15.6
400 / 2$\bar{2}$0	7.5	5.3
220	14.5	7.1
510 / 420	14.1	16.0
130	7.9	14.9
600 / 3$\bar{3}$0	10.0	9.9
330	6.7	12.4

[a] For the pairs of (200) and (1$\bar{1}$0), (400) and (2$\bar{2}$0), etc., the overlapping of reflections was assumed (refer to *Figure 17*)
[b] Calculated structure factors are for the model with statistical weight of 60°-rotated chains w = 27.3%. An isotropic temperature parameter B = 10.0 $Å^2$ was assumed for all the atoms

relative amount of *trans* bonds, is not practically reduced, though slight reduction may be detected. From these experimental facts (a)–(d) the molecular structure of the cooled phase may be considered to be constructed principally by long *trans* sequences and by a little bit of some other rotational isomers as a disorder. The inclusion of the latter may induce a small expansion of the unit cell, a slight contraction of the fibre period and X-ray diffuse scattering. When such chains are tensioned along the fibre axis, a complete transformation of rotational isomers into *trans* state will occur and then the chain will have an all-*trans* conformation (the low-temperature phase). Additional experimental facts to be considered are as follows. (e) The X-ray intensity calculation indicates the existence of *trans* chains pointing their dipoles into 0° and 60° directions from the b-axis with almost equal probability. As discussed before, this suggests the possibility of an appreciable amount of 60° domain structure more clearly than the case of the low-temperature phase. (f) The zigzag chains tilt about 18° within the (130) plane. As seen from *Figure 12*, the zigzag chains located at the centre and corners of the unit cell

belong to the adjacent (130) planes separately. These structural features may suggest the role of (130) plane in formation of domain structure and occurrence of tilting phenomenon as will be explained later. In the low-temperature phase the tilt angle is reduced to about 3°.

We have tried to find a structural model of the cooled phase suitable to explain all the experimental facts (a)–(f) consistently. We now speculate the molecular structural change occurring in the cooling process from the high-temperature phase as shown in *Figure 19*. Here the molecular conformation of the high-temperature phase is simplified by $T_3GT_3\bar{G}$ regular form. In *Figure 19* the rotational isomeric change from *gauche* to *trans* is assumed to occur successively in the vicinity of the transition temperature *via skew form*[36]. Below the transition temperature some part of chain sequence are assumed not to proceed completely to the all-*trans* structure but to be frozen-in at a stage of the skew structure, that is:

$$\ldots TTTTTTTTT\bar{S}TTTTTTTTTT\bar{S}TTTTTT\ldots$$

The *trans* chain segments in such a conformational model tilt by about 16° from the vertical line, as shown in *Figure 20*. Following the experimental fact (f), if *trans* segments of the cooled phase are tilted by about 18° in the (130) plane of the basic structure of *Figure 12*, the resultant structure corresponds well to the present model. In this 'bent *trans* model' the CF_2 dipoles of two successive *trans* segments make an angle 60° to each other. By exchanging the bond S into $\bar{S}$ or up-and-down inversion of chain direction, we can generate other bent *trans* chains with dipoles pointing in other 60° directions and these chains can be overlapped in a statistical fashion as indicated by solid and broken lines in *Figure 20a*. If these chains are packed together in parallel, the resultant crystal will have a subcell structure of *Figure 20a*, i.e. the 0° and ±60° rotated *trans* chains are statistically placed at one lattice point and the unit cell tilts by about 16° in the (130) plane. This is just the structure model revealed by the X-ray analysis. In other words, the tilting phenomenon and the 60° domain structure may be a result necessarily induced by the generation of skew bonds within the long *trans* sequences. In *Figure 20b* is shown the posible local structure of three-dimensionally developed 60° domains, where the domains are bounded by the (130) plane in the horizontal direction and by the skew linkages in the vertical direction. The size of the domains might vary from place to place, and the resultant random distribution of the skew bonds will cause the X-ray diffuse scattering as stated in experimental fact (c). Drawing the cooled phase by a few per cent of strain gives the low-temperature phase, in which the tilt angle and the probability of 60° domain structure are reduced largely from the values for the cooled phase. The molecular chain containing skew bonds may transfer to the all-*trans* conformation by the stress-induced internal rotation change. As a result the *trans* segments will stand up more vertically and most of the CF_2 dipoles become parallel to each other. In other words, a more regular and single-domain-like structure may be obtained by drawing.

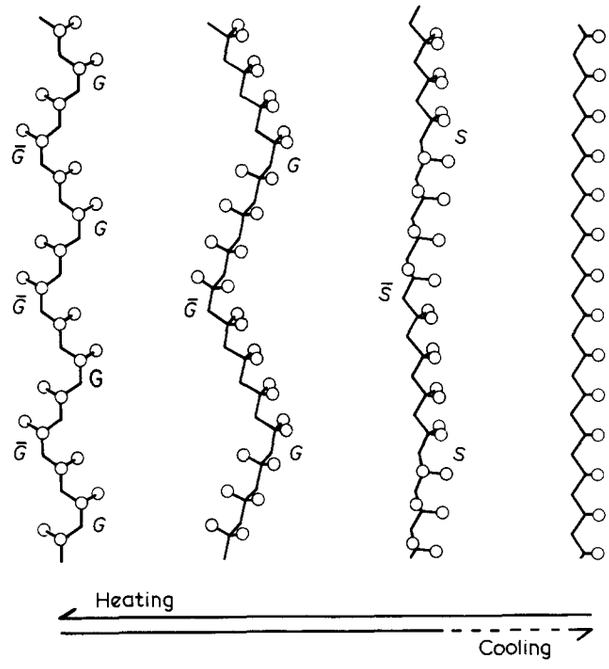

Figure 19 Transitional model of single molecular chain of VDF 55% copolymer, where the monomeric unit is simplified by CH_2CF_2 unit for convenience

In the actual sample of the cooled phase there may also exist another kind of disorder. For example, the kink structure of *gauche* segments contained within the *trans* sequence may also result in the X-ray diffuse scattering[37] and the slight decrease in infra-red absorbance of *trans* bands. These *gauche* bonds may also shorten the fibre period of the *trans* chain on average.

Our structural model for the cooled phase is supported also from energetic considerations. Hopfinger *et al.*[38,39] investigated the effect of head-to-head and tail-to-tail (hhtt) abnormal linkages on the conformational stability of a PVDF chain by energy calculations and clarified that as the hhtt linkages increase the *trans* conformation becomes more stable than the $TGT\bar{G}$ conformation. For hhtt linkage of about 20%, for example, the energy of the all-*trans* conformation is lower by about 5 kcal mol^{-1} than that of $TGT\bar{G}$. In this case the existence of an intermediately stable $TST\bar{S}$ form also becomes possible (*Figure 21*). The possible existence of two energetically stable conformations, $TTTT$ and $TST\bar{S}$, for the VDF polymer with 20% hhtt abnormal bonds allows us to predict the stable appearance of above-mentioned long *trans* chains containing skew bonds. Hopfinger *et al.* also stated that the effect of introducing a TrFE unit into the VDF sequences may be equivalent to about a half in magnitude of the effect of hhtt linkage[38,39]. Thus the 20% hhtt may correspond to 40% TrFE or the VDF–TrFE copolymer with VDF molar ratio of 60%. That is to say, it might be possible to discuss the energetics of VDF 55% copolymer chain based on the potential energy curve calculated for VDF polymer having hhtt likage of 20%; the heating of low-temperature phase of VDF 55% copolymer transfers the stable all-*trans* form to the *gauche* one *via the trans conformation containing the skew linkages*. On the cooling process the *gauche* conformation does not transfer back completely to the energetically most stable all-*trans* conformation but the intermediately stable skew form is frozen-in. The speculation just mentioned may be quite consistent with the transition scheme of *Figure 4*. The detailed conformational analysis for our structure model will be reported elsewhere.

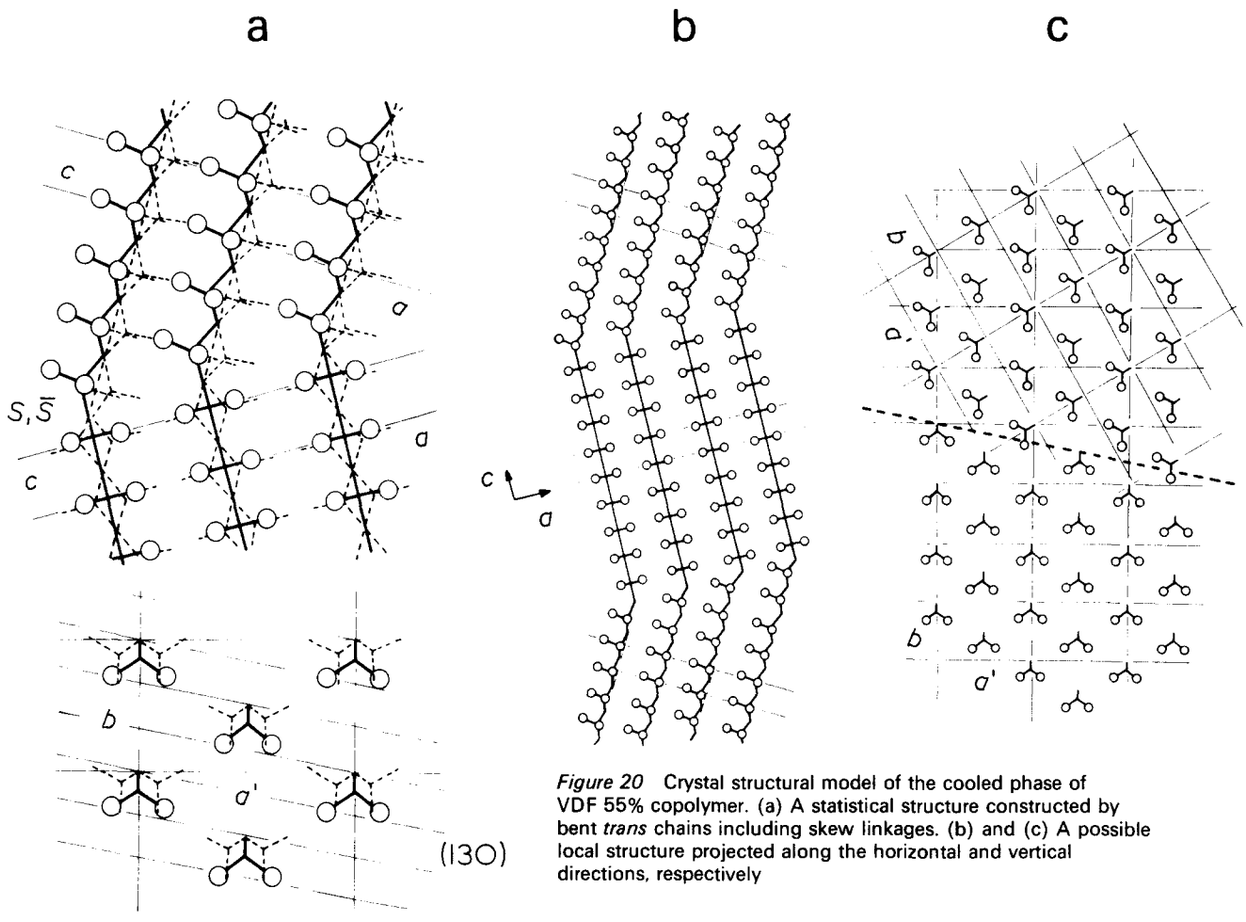

Figure 20 Crystal structural model of the cooled phase of VDF 55% copolymer. (a) A statistical structure constructed by bent *trans* chains including skew linkages. (b) and (c) A possible local structure projected along the horizontal and vertical directions, respectively

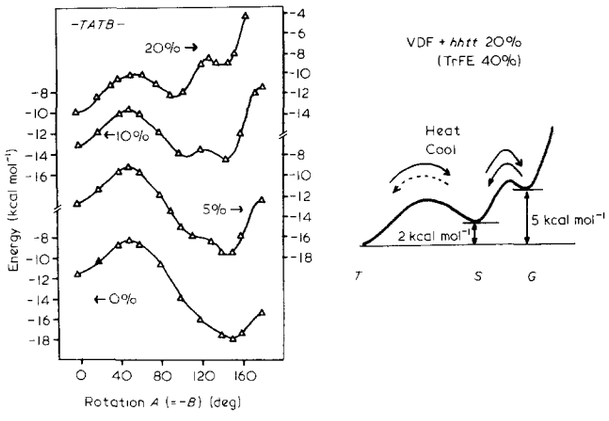

Figure 21 (a) Potential energy curves for poly(vinylidene fluoride) chain including randomly head-to-head and tail-to-tail abnormal linkages in a certain per cent (after Hopfinger *et al.*[38,39]). (b) The energy curve for the hhtt linkage of 20% which corresponds to the case of 40% TrFE according to Hopfinger *et al.*

CONCLUSION

Crystal structural change in ferroelectric phase transition of VDF 55% copolymer may be described as follows. The low-temperature phase consists of the parallel arrangement of dipoles of all-*trans* zigzag chains and so it is a polar crystal. As the temperature rises near the transition point, a new crystal phase (cooled phase) appears and coexists with the original low-temperature phase. In this new phase, the skew bonds generated within the long *trans* chains induce necessarily a tilting of the long *trans* segments by about 18° in the (130) plane. As the temperature rises further, the *gauche* bonds increase rapidly and the molecular chain transfers continuously to the conformation of the high-temperature phase, constructed by a random combination of TG, $T\bar{G}$, T_3G and $T_3\bar{G}$ isomers. These chains experience a large rotational motion around the chain axis due to thermal agitation. In the cooling process the transformation from *gauche* to *trans* isomers occurs cooperatively but some bonds are frozen-in in the metastable skew form and the cooled phase is obtained at room temperature, where the *trans* segments are tilted and the 60° domain structure is constructed because of the existence of skew bonds. Mechanical drawing of the cooled phase transfers the skew bond into the *trans* bond and then the low-temperature phase is obtained, where the all-*trans* chains are regularly packed and the probability of 60° domain structure is also reduced.

As the VDF content of the copolymer increases to higher value the transitional behaviour becomes rather simple[24]. For example, in the case of VDF 72% copolymer, the first-order transition between the all-*trans* low-temperature phase and the *gauche* high-temperature phase can be clearly observed at a temperature of about 130°C. On the other hand, the copolymer with the lower VDF content shows rather obscure phase transition; for example, the VDF 37% copolymer transforms slowly between the cooled phase and the high-temperature phase in a wide temperature range from 0° to 80°C. Such a difference in transitional behaviour might originate from

the difference in the length of the regular VDF monomer sequences among the copolymers with different VDF contents. The detailed experimental results will be reported soon.

ACKNOWLEDGEMENT

The authors are grateful to Drs Syun Koizumi, Junichi Sako, Toshiharu Yagi and Yoshihide Higashihata of Daikin Kogyo Co. Ltd. for supplying samples of VDF–TrFE copolymers.

REFERENCES

1 Kepler, R. G. and Anderson, R. A. *J. Appl. Phys.* 1978, **49**, 1232
2 Takahashi, N. and Odajima, A. *Ferroelectrics* 1981, **49**, 49
3 Tasaka, S. and Miyata, S. *Polym. Prepr. Jpn.* 1982, **31**, 2317
4 Naegele, D. and Yoon, D. Y. *Appl. Phys. Lett.* 1978, **33**, 132
5 Takahashi, T., Date, M. and Fukada, E. *Appl. Phys. Lett.* 1980, **37**, 791
6 Tashiro, K., Itoh, Y., Kobayashi, M. and Tadokoro, H. *Polym. Prepr. Jpn.* 1980, **29**, 2067
7 *Ferroelectrics* 1980, **32**, Special issue on ferroelectricity of PVDF
8 Buchman, P. *Ferroelectrics* 1975, **5**, 39
9 Matsushige, K., Imada, S. and Takemura, T. *Polym. J.* 1981, **13**, 493
10 Furukawa, T. and Johnson, G. E. *Appl. Phys. Lett.* 1981, **38**, 1027
11 Takase, Y. and Odajima, A. *Polym. Prepr. Jpn.* 1982, **31**, 2915
12 Nakamura, K. and Wada, Y. *J. Polym. Sci. A-2* 1971, **9**, 161
13 Micheron, F. *Ferroelectrics* 1980, **28**, 395
14 Herchenröder, P., Segui, Y., Horne, D. and Yoon, D. Y. *Phys. Rev. Lett.* 1980, **45**, 2135
15 Tashiro, K., Takano, K., Kobayashi, M., Chatani, Y. and Tadokoro, H. *Polymer* 1983, **24**, 199
16 Yagi, T., Tatemoto, M. and Sako, J. *Polym. J.* 1980, **12**, 209
17 Higashihata, Y., Sako, J. and Yagi, T. *Ferroelectrics* 1981, **32**, 85
18 Kitayama, T., Ueda, T. and Yamada, T. *Ferroelectrics* 1980, **28**, 301
19 Furukawa, T., Date, M., Fukada, E., Tajitsu, Y. and Chiba, A. *Jpn. J. Appl. Phys.* 1980, **19**, L109
20 Tajitsu, Y., Chiba, A., Furukawa, T., Date, M. and Fukada, E. *Appl. Phys. Lett.* 1980, **36**, 286
21 Furukawa, Y., Johnson, G. E., Bair, H. E., Tajitsu, Y. and Chiba, A. *Ferroelectrics* 1981, **32**, 61
22 Tashiro, K., Takano, K., Kobayashi, M., Chatani, Y. and Tadokoro, H. *Polymer* 1981, **22**, 1312
23 Lines, M. E. and Glass, A. M. 'Principles and Applications of Ferroelectrics and Related Materials', Oxford University Press, London, 1977
24 Tashiro, K., Takano, K., Kobayashi, M., Chatani, Y. and Tadokoro, H. *Polym. Prepr. Jpn.* 1982, **31**, 2887
25 Lovinger, A. J. *Macromolecules* 1982, **15**, 40
26 Lovinger, A. J., Davis, G. T., Furukawa, T. and Broadhurst, M. G. *Macromolecules* 1982, **15**, 323
27 Davis, G. T., Furukawa, T., Lovinger, A. J. and Broadhurst, M. G. *Macromolecules* 1982, **15**, 329
28 Hasegawa, R., Takahashi, Y., Chatani, Y. and Tadokoro, H. *Polym. J.* 1972, **3**, 600
29 Tadokoro, H. 'Structure of Crystalline Polymers', John Wiley & Sons, New York, 1979
30 Weinhold, S., Litt, M. H. and Lando, J. B. *Macromolecules* 1980, **13**, 1178
31 Takahashi, Y. and Tadokoro, H. *Macromolecules* 1980, **13**, 1317
32 Kobayashi, M., Tashiro, K. and Tadokoro, H. *Macromolecules* 1975, **8**, 158
33 Tashiro, K., Kobayashi, M. and Tadokoro, H. *Macromolecules* 1981, **14**, 1757
34 Yagi, T. and Tatemoto, M. *Polym. J.* 1979, **11**, 429
35 Daubeny, R. de P., Bunn, C. W. and Brown, C. J. *Proc. R. Soc. A* 1954, **226**, 531
36 Takahashi, Y., Matsubara, Y. and Tadokoro, H. *Macromolecules* 1982, **15**, 334
37 Takahashi, Y. and Tadokoro, H. *Macromolecules* 1980, **13**, 1318
38 Farmer, B. L., Hopfinger, A. J. and Lando, J. B. *J. Appl. Phys.* 1972, **43**, 4293
39 Hopfinger, A. J. 'Conformational Properties of Macromolecules', Academic Press, New York, 1973